Time-Dependent Density Functional Study of Electroluminescent Polymers

Jen-Shiang K. Yu, Wei-Chen Chen, and Chin-Hui Yu*

Department of Chemistry, National Tsing Hua Universtity, Hsinchu 300, Taiwan

Received: July 8, 2002; In Final Form: December 3, 2002

The theoretical spectra of electroluminescent polymers are studied with time-dependent density functional theories, followed by a systematic scheme with a symmetry restriction to extrapolate the absorption and emission corresponding to infinite chains avoiding periodic boundary conditions. Application to poly(*p*-phenylene vinylene) (PPV) and the derivatives has been attempted, and the hybrid B3LYP is concluded to be the most suitable functional for computation. The theoretical excitation energies of PPV by B3LYP/6-31G*//B3LYP/STO-3G and B3LYP/6-311G* are 2.107 and 2.027 eV, respectively. With optimization performed by single-excited configuration interaction, the emission spectroscopy can be estimated. By our scheme, the Stokes shift of PPV is calculated to be 0.223 eV, which corresponds to approximately 62 nm in the spectral region.

Introduction

A recent review[1] has summarized that the properties of many solid-state organic materials are of interest for their distinguished optical, electrical, photoelectric, and magnetic characteristics. These materials with photo and electric activities have been studied extensively, aiming at potential applications of device fabrication. Amorphous molecular materials have been discovered to be of successful utilization in the domain of organic electroluminescent (EL) devices and are continually being explored. The organic EL compounds have been candidate materials for color flat-panel displays because of low driving voltage, high brightness, capability of multicolor emission by the selection of emitting materials, and easy fabrication of large-area and thin-film devices. Pioneering work for EL devices featuring the single crystals of anthracene was done by Pope et al.,[2] followed by Bradley et al.,[3] with the use of conjugated polymer poly(*p*-phenylene vinylene) (PPV). These pilot studies have triggered widespread research and development of this field. To date, the conjugated polymeric derivatives remain one of the most popular target materials for the EL devices.

A theoretical investigation of PPV was first done by Gomes da Costa et al.[4] with the local density functional method to calculate the 3D band structure. The geometric, electronic, and optical properties of the derivatives of the PPV oligomers reported by Cornil et al.[5] provided rough insight into the relationship between the emitting red/blue shift and the effect of substituent groups of the PPV derivatives. The geometry optimizations on the nine oligomers employed the semiempirical Hartree−Fock Austin model 1 (AM1)[6] method, followed by the energy calculations using the intermediate neglect of differential overlap (INDO) Hamiltonian[7] and a single configuration interaction (SCI) scheme[8] of single excitation up to the 20 highest occupied and 20 lowest unoccupied molecular orbitals. The energy bands and bond alternation potential in PPV were studied by Fröner et. al.[9] with comparative ab initio quantum chemical and density functional theories. The local density approximation[10] (LDA), the Hartree−Fock (HF) method, and the second-order Møller−Plesset perturbation (MP2) theories were utilized, and the correlation-correction band gap is 2.7 eV. The most recent first principles study of PPV and its derivatives was done by Vaschetto and Springborg[11] using a parameter-free density functional method (DFT-LMTO-full potential). The theoretical band gap obtained for PPV is 2.1 eV.

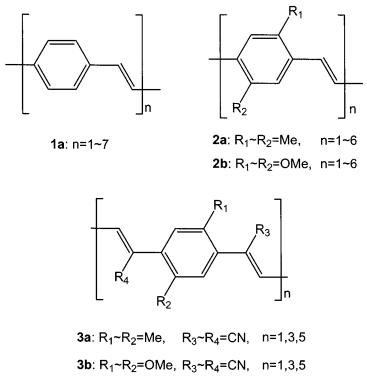

Figure 1. General structures of PPV (**1a**) and methyl- and methoxy-substituted PPV (**2a** and **2b**) as well as their nitriles (**3a** and **3b**).

It would be possible to conduct molecular design and color tuning by computers as the absorption and emission spectra of EL materials are accurately evaluated by theoretical methods. We investigate the spectral properties of the PPV and its derivatives by time-dependent density functional theories (TD-DFT)[12] avoiding periodic boundary conditions. Calculations have been made for PPV*n* oligomers where *n* is the number of units, and up to 7 have been employed in the present study.[13]

Theoretical Models and Calculations

The general structures of the original PPV polymer and its derivatives are shown in Figure 1. The scheme of **1a** is the original structure of PPV, whereas **2a** and **2b** denote the methyl- and methoxy-substituted PPVs, respectively. The structures of **3a** and **3b** are the nitriles of corresponding **2a** and **2b**. One hydrogen atom and a $-CH{=}CH_2$ group are added individually at each end of these polymerized units of **1a**, **2a**, and **2b** to

* Corresponding author. E-mail: chyu@oxygen.chem.nthu.edu.tw. Fax: +886-3-5721534.

10.1021/jp026461j CCC: $25.00
Published on Web 04/30/2003

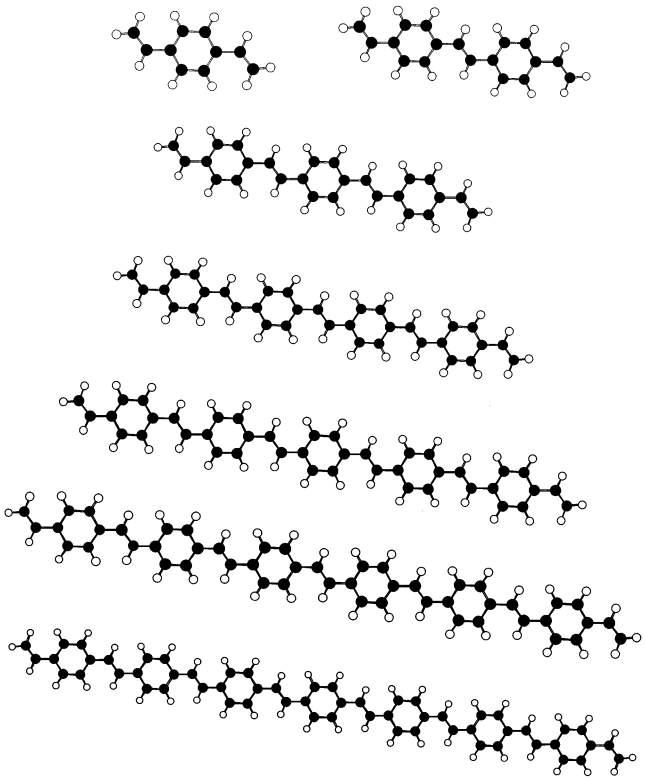

Figure 2. Modeling structures of PPV (**1a**) monomer through heptamer.

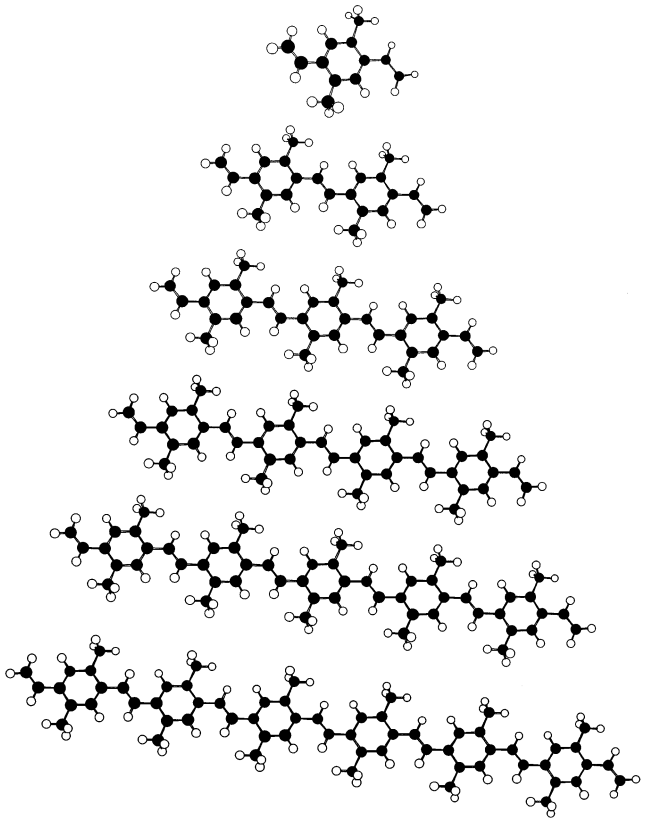

Figure 3. Modeling structures of methyl-substituted PPV (**2a**) monomer through hexamer.

constrain the C_{2h} symmetry during the geometry optimizations and TD energy calculations. Two terminal hydrogen atoms are separately attached as well to **3a** and **3b** for the concern of the identical symmetry constraint. This symmetry-constrained linear extrapolation (SCLE) for excitation energy using TD-DFT can utilize various density functionals and is abbreviated as SCLE-TD-DFT later in the text.

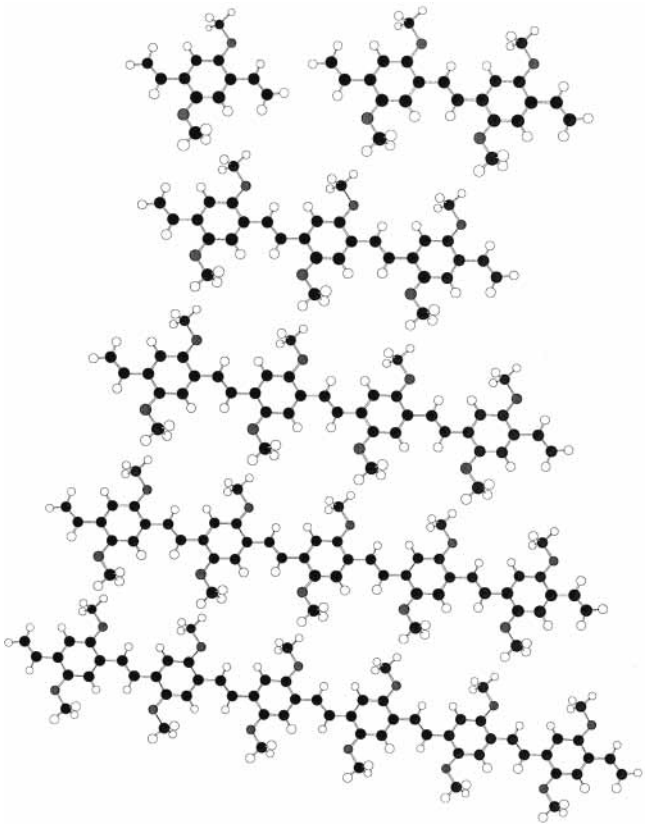

Figure 4. Modeling structures of methoxy-substituted PPV (**2b**) monomer through hexamer.

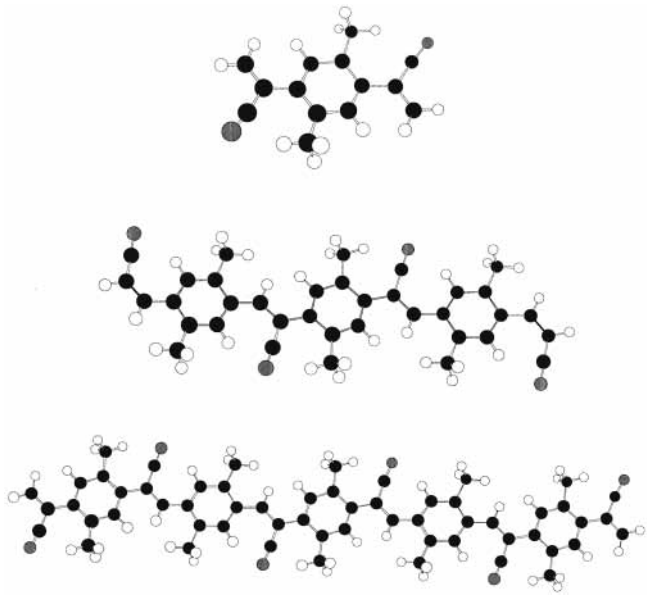

Figure 5. Modeling structures of methyl-substituted PPV nitrile (**3a**) monomer, trimer, and pentamer.

The actual geometries of the PPV monomer through the heptamer are shown in Figure 2. The Gaussian 98 program[14] compiled by the Intel Fortran Compiler[15] has been used for the density functional calculations in 32-bit PC-Linux systems. Jobs with scratch files larger than 16 GB were performed by Compaq Alpha workstations. The density functional theories that were used include nonhybrid methods such as BP86[16] and BLYP[17] and hybrid-type B3LYP[18] theories. The geometry optimizations are first done using the STO-3G basis set with each DFT

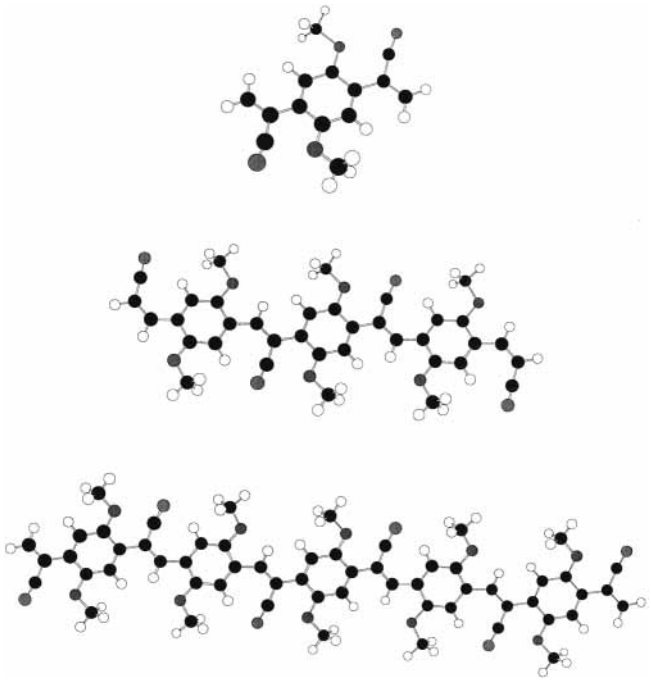

Figure 6. Modeling structures of methoxy-substituted PPV nitrile (**3b**) monomer, trimer, and pentamer.

TABLE 1: Stoichiochemical Formulas of the Modeling PPV (1a) Monomer through Heptamer as Well as the Numbers of Basis Functions of Corresponding Basis Sets

modeling oligomers	stoichiochemistry	number of basis functions			
		STO-3G	3-21G	4-31G*	6-31G*
monomer	$C_{10}H_{10}$	60	110	170	170
dimer	$C_{18}H_{16}$	106	194	302	302
trimer	$C_{26}H_{22}$	152	278	434	434
quadmer	$C_{34}H_{28}$	198	362	566	566
pentamer	$C_{42}H_{34}$	244	446	698	698
hexamer	$C_{50}H_{40}$	290	530	830	830
heptamer	$C_{58}H_{46}$	336	614	962	962
n	$C_{8n+2}H_{6n+4}$				

method, followed by the time-dependent computations up to the first five singlet and five triplet states using STO-3G, 3-21G, 4-31G*, and 6-31G* basis sets, respectively. Spectroscopic data for infinite chains of the polymers were determined by plotting corresponding transitions against the reciprocal of the number of modeling polymeric units and by extrapolating the number of units to infinity.[13] The effects of basis sets were verified by similar calculations performed using 6-31G* and triple-ζ 6-311G* basis sets to optimize the geometries followed by the TD scheme mentioned above.

The excitation spectra by SCLE-TD-DFT for **2a** and **2b** are based on their monomers through hexamers; the structrues are shown in Figures 3 and 4. Likewise, theoretical absorptions for **3a** and **3b** were performed by the combination of [monomer−trimer−pentamer] modeling units, and the structures are demonstrated in Figures 5 and 6. The stoichiochemistry and generic formulas for the aforementioned modeling oligomers, as well as their corresponding numbering description of these original and substituted PPV oligomers, are summarized in Tables 1 and 2 in detail.

Results and Discussion

Excitation Energy of PPV. The SCLE-TD excitation energies for PPV oligomers using BP86, BLYP, and B3LYP density functional methods with STO-3G, 3-21G, 4-31G*, and 6-31G* basis sets are tabulated in Tables 3−5, whereas the linear regression plots for their first active TD excitations are displayed in Figures 7−9. All of the ground states are the ^1A_g state, whereas the excited states with nonzero oscillator strengths all belong to the ^1B_u state. Considering the linearity, Figure 7 shows that the correlation coefficient obtained by the SCLE-BP86-TD method is at least 0.910. Utilizing the largest basis set of 6-31G*, SCLE-BP86 gives an excitation energy of 1.470 eV with a correlation coefficient of 0.992. In Figure 8, the SCLE-BLYP method with the largest 6-31G* basis set gives an excitation energy of 1.438 eV and a correlation coefficient of 0.990. Because the experimental band gap is 2.2 eV,[3] the BP86 and BLYP functionals both obviously underestimate the excitation energy of PPV.

The regression data shown in Figure 9 offer relatively the best correlation coefficient and the closest excitation energy to the experimental data. The calculation at the level of SCLE-

TABLE 2: Stoichiochemistry Formulas of the Models of Substituted PPV Polymers (2a, 2b, 3b, and 3b) as Well as the Number of Basis Functions of Corresponding Basis Sets

schemes	PPV substituents	modeling oligomers	units *n*	stoichiochemistry	number of basis functions	
					STO-3G	6-31G*
2a	(di)methyl	monomer	1	$C_{12}H_{14}$	74	208
		dimer	2	$C_{22}H_{24}$	134	378
		trimer	3	$C_{32}H_{34}$	194	548
		quadmer	4	$C_{42}H_{44}$	254	718
		pentamer	5	$C_{52}H_{54}$	314	888
		hexamer	6	$C_{62}H_{64}$	374	1058
			n	$C_{10n+2}H_{10n+4}$		
2b	(di)methoxy	monomer	1	$C_{12}H_{14}O_2$	84	238
		dimer	2	$C_{22}H_{24}O_4$	154	438
		trimer	3	$C_{32}H_{34}O_6$	224	638
		quadmer	4	$C_{42}H_{44}O_8$	294	838
		pentamer	5	$C_{52}H_{54}O_{10}$	364	1038
		hexamer	6	$C_{62}H_{64}O_{12}$	434	1238
			n	$C_{10n+2}H_{10n+4}O_{2n}$		
3a	(di)methyl-(di)cyano	monomer	1	$C_{14}H_{12}N_2$	92	264
		trimer	3	$C_{36}H_{30}N_4$	230	660
		pentamer	5	$C_{58}H_{48}N_6$	368	1056
			n	$C_{11n+3}H_{9n+3}N_{n+1}$		
3b	(di)methoxy-(di)cyano	monomer	1	$C_{14}H_{12}N_2O_2$	102	294
		trimer	3	$C_{36}H_{30}N_4O_6$	260	750
		pentamer	5	$C_{58}H_{48}N_6O_{10}$	418	1206
			n	$C_{11n+3}H_{9n+3}N_{n+1}O_{2n}$		

TABLE 3: SCLE-TD Excitation Energies (E_{ex}, eV) of PPV (1a) with Nonzero Oscillator Strengths (f) of the $^1B_u \leftarrow A_g$ Transition by the BP86 Density Functional[a]

polymer units (n)	SCLE-TD-BP86/STO-3G//BP86/STO-3G						SCLE-TD-BP86/3-21G//BP86/STO-3G					
	first		second		third		first		second		third	
	E_{ex}	f	E_{ex}	f	E_{ex}	f	E_{ex}	f	E_{ex}	f	E_{ex}	f
1	4.8156	0.0456	4.8646	0.6873			4.1095	0.5889	4.2621	0.0453		
2	3.5538	1.4524	3.9967	0.0044			3.0383	1.3749	3.5673	0.0016	3.8288	0.0254
3	2.9352	1.8649	3.6852	0.0916	3.8607	0.7009	2.5093	1.8799	3.3705	0.0758	3.3777	0.4846
4	2.5898	2.0738	3.2340	0.1193	3.2777	1.1178	2.2016	2.1755	2.8635	0.1126	2.8648	0.8907
5	2.3775	2.1715	2.8539	0.1247	2.9271	1.5158	2.0019	2.3508	2.5307	0.1270		
6	2.2390	2.2053	2.5887	0.1233	2.6934	1.8562	1.8693	2.4400	2.3046	0.1304		
7	2.1444	2.2081	2.4412	0.1253	2.5227	2.1200	1.8818	2.3371	2.2219	0.1455	2.2468	1.9802
∞	1.794	(0.993)	2.494	(0.933)			1.527	(0.992)	2.118	(0.910)		
	SCLE-TD-BP86/4-31G*//BP86/STO-3G						SCLE-TD-BP86/6-31G*//BP86/STO-3G					
polymer units (n)	first		second		third		first		second		third	
	E_{ex}	f	E_{ex}	f	E_{ex}	f	E_{ex}	f	E_{ex}	f	E_{ex}	f
1	3.9945	0.5696	4.1566	0.0383			3.9588	0.5598	4.1378	0.0412		
2	2.9554	1.3401	3.4483	0.0016	3.7125	0.0284	2.9346	1.3345	3.4394	0.0016	3.6870	0.0303
3	2.4393	1.8462	3.2802	0.0797	3.3497	0.0081	2.4232	1.8474	3.2575	0.0708	3.2644	0.4480
4[b]							2.1233	2.1535	2.7701	0.1088		
5	1.9410	2.3260	2.4535	0.1310			1.9276	2.3383	2.4387	0.1187		
6	1.8103	2.4205	2.2266	0.1296			1.7971	2.4364	2.2155	0.1168		
7	1.8206	2.3239	2.1395	0.1412			1.8067	2.3409	2.1283	0.1275		
∞	1.476	(0.992)	2.076	(0.911)			1.470	(0.992)	2.091	(0.911)		

[a] The geometries are optimized at the BP86/STO-3G level of theory, followed by the TD calculations up to the first five singlet and five triplet states. The excitation energies for $n = \infty$ correspond to infinite numbers of polymer units by linear regression. The numbers in parentheses are the correlation constants (r). [b] Numerically failed to converge for an optimal structure.

TABLE 4: SCLE-TD Excitation Energies (E_{ex}, eV) of PPV (1a) with Nonzero Oscillator Strengths (f) of the $^1B_u \leftarrow {}^1A_g$ Transition by the BLYP Density Functional[a]

polymer units (n)	SCLE-TD-BLYP/STO-3G//BLYP/STO-3G						SCLE-TD-BLYP/3-21G//BLYP/STO-3G					
	first		second		third		first		second		third	
	E_{ex}	f	E_{ex}	f	E_{ex}	f	E_{ex}	f	E_{ex}	f	E_{ex}	f
1	4.7277	0.0333	4.7812	0.6824	5.0731	0.0807	4.0726	0.5756	4.2089	0.0503		
2	3.4958	1.4241	3.9242	0.0042			3.0143	1.3532	3.5330	0.0016		
3	2.8921	1.8231	3.6197	0.0892	3.7643	0.6873	2.4914	1.8426	3.3349	0.0748	3.3720	0.5048
4	2.5541	2.0238	3.1736	0.1145	3.2253	1.1119	2.1863	2.1296	2.8340	0.1067	2.8362	0.9023
5	2.3477	2.1166	2.8040	0.1188	2.8835	1.5030	1.9934	2.2891	2.5111	0.1187		
6	2.2128	2.1484	2.5459	0.1172	2.6552	1.8353	1.8638	2.3724	2.2895	0.1212		
7	2.1215	2.1453	2.4000	0.1196	2.4896	2.0913	1.7741	2.4105	2.1165	0.1227		
∞	1.763	(0.994)	2.372	(0.961)			1.494	(0.991)	2.131	(0.920)		
	SCLE-TD-BLYP/4-31G*//BLYP/STO-3G						SCLE-TD-BLYP/6-31G*//BLYP/STO-3G					
polymer units (n)	first		second		third		first		second		third	
	E_{ex}	f	E_{ex}	f	E_{ex}	f	E_{ex}	f	E_{ex}	f	E_{ex}	f
1	3.9626	0.5584	4.1075	0.0426			3.9263	0.5483	4.0877	0.0453		
2	2.9347	1.3212	3.4201	0.0016	3.6765	0.0279	2.9132	1.3156	3.4106	0.0015	3.6498	0.0299
3	2.4240	1.8126	3.2486	0.0782	3.2507	0.4683	2.4071	1.8139	3.2257	0.0692	3.2315	0.4603
4	2.1245	2.1040	2.7548	0.1122	2.7580	0.8662	2.1094	2.1116	2.7373	0.1011	2.7428	0.8614
5	1.9344	2.2684	2.4367	0.1210			1.9200	2.2807	2.4208	0.1088		
6	1.8064	2.3571	2.2179	0.1192			1.7922	2.3728	2.2047	0.1066		
7	1.7175	2.4002	2.0434	0.1165	2.0652	1.9824	1.7034	2.4184	2.0316	0.1040		
∞	1.447	(0.991)	2.075	(0.907)			1.438	(0.990)	2.055	(0.906)		

[a] The geometries are optimized at the BLYP/STO-3G level of theory, followed by the TD calculations up to the first five singlet and five triplet states. The excitation energies for $n = \infty$ correspond to infinite numbers of polymer units by linear regression. The numbers in parentheses are the correlation constants (r).

TD-B3LYP/6-31G*//B3LYP/STO-3G suggests that the $^1B_u \leftarrow {}^1A_g$ excitation energy of PPV is 2.107 eV with a correlation coefficient (r) of 0.996, which is close to the observed optical absorption edge and agrees well with the previous theoretical result of 2.1 eV from the parameter-free DFT-LMTO-full potential by Vaschetto and Springborg[11] as well as the experimental value of 2.2 eV.[3] Therefore, with our modeling system, the SCLE-TD-B3LYP/6-31G* method will be the most suitable functional to estimate the absorption energy, and it is employed throughout the computations for all of the following electronic transitions.

To verify the effect of basis sets, additional geometrical minimizations were performed using larger basis sets such as 6-31G* and triple-ζ 6-311G* in conjunction with the B3LYP functional for PPV polymers as well as selected substituted oligomers, followed by TD excitations at identical levels of

TABLE 5: SCLE-TD Excitation Energies (E_{ex}, eV) of PPV (1a) with Nonzero Oscillator Strengths (f) of the $^1B_u \leftarrow {}^1A_g$ Transition by the B3LYP Density Functional[a]

polymer units (n)	SCLE-TD-B3LYP/STO-3G//B3LYP/STO-3G						SCLE-TD-B3LYP/3-21G//B3LYP/STO-3G					
	first		second		third		first		second		third	
	E_{ex}	f	E_{ex}	f	E_{ex}	f	E_{ex}	f	E_{ex}	f	E_{ex}	f
1	5.3251	0.1707	5.3355	0.6667	6.2150	0.1512	4.4897	0.6757	4.7025	0.0367		
2	4.1277	1.7180					3.4789	1.5553				
3	3.6001	2.4299					3.0233	2.3044	4.0231	0.0041	4.0451	0.0206
4	3.3286	3.0516					2.7785	2.9762	3.5454	0.0462	3.5918	0.4385
5	3.1710	3.6431	3.8121	0.1286	3.8302	0.5984	2.6315	3.6139	3.3148	0.1229		
6	3.0721	4.2323	3.5349	0.7642			2.5369	4.2412	3.1143	0.3038		
7	3.0112	4.8322					2.4766	4.8738	2.8495	0.5566		
∞	2.650	(0.998)	3.111	(0.998)			2.185	(0.996)	2.949	(0.903)		

polymer units (n)	SCLE-TD-B3LYP/4-31G*//B3LYP/STO-3G				SCLE-TD-B3LYP/6-31G*//B3LYP/STO-3G			
	first		second		first		second	
	E_{ex}	f	E_{ex}	f	E_{ex}	f	E_{ex}	f
1	4.3657	0.6518	4.5954	0.0307	4.3229	0.6388	4.5697	0.0346
2	3.3860	1.5179			3.3580	1.5068		
3	2.9419	2.2678			2.9180	2.2584		
4	2.7023	2.9452	3.4961	0.0445	2.6799	2.9375	3.4770	0.0382
5	2.5581	3.5907	3.2430	0.1224	2.5362	3.5841	3.2230	0.1113
6	2.4648	4.2269			2.4431	4.2206		
7	2.4053	4.8681			2.3836	4.8616		
∞	2.123	(0.996)	3.008	(0.993)	2.107	(0.996)	2.991	(0.992)

[a] The geometries are optimized at the B3LYP/STO-3G level of theory, followed by the TD calculations up to the first five singlet and five triplet states. The excitation energies for $n = \infty$ correspond to infinite numbers of polymer units by linear regression. The numbers in parentheses are the correlation constants (r).

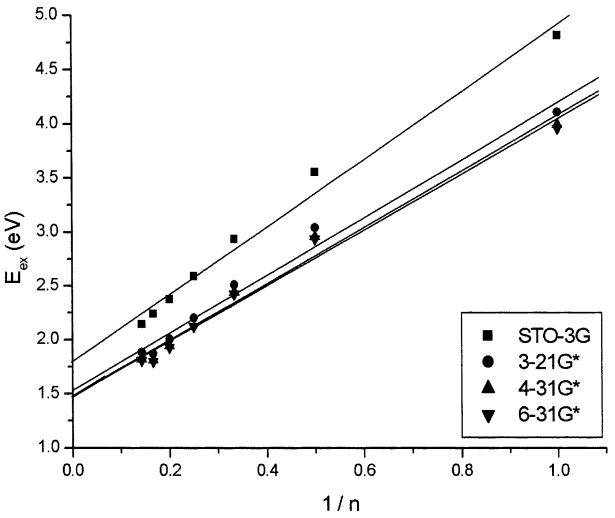

Figure 7. Excitation energy (E_{ex}, eV) of PPV (**1a**) by the SCLE-TD-BP86 method with various basis sets. The structures are optimized at the level of BP86/STO-3G.

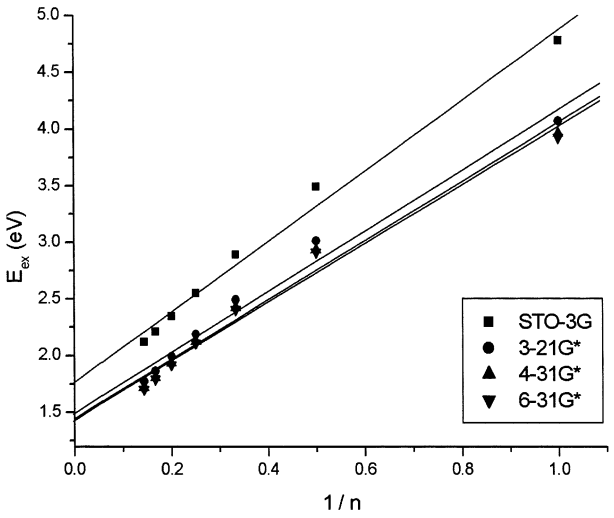

Figure 8. Excitation energy (E_{ex}, eV) of PPV (**1a**) by the SCLE-TD-BLYP method with various basis sets. The structures are optimized at the level of BLYP/STO-3G.

theory to those of the optimizations. From these computations at higher levels displayed in Table 6, the deviation of the regressive TD band gap of PPV between B3LYP/6-31G*//B3LYP/STO-3G and B3LYP/6-311G*//B3LYP/6-311G* is 0.08 eV, which corresponds to approximately 23 nm of the spectral shift (<4%) in this range. Excitation energies tend to converge with the size of basis sets. Considering the computational resource requirement, it is feasible to study these polymers with the TD-B3LYP/6-31G*//B3LYP/STO-3G theory with both efficiency and acceptable accuracy.

Excitation Energies of Substituted PPVs. In Table 7, the TD-B3LYP band gaps of selected derivatives obtained with larger basis sets such as TD-B3LYP/6-31G*//B3LYP/6-31G* and TD-B3LYP/6-311G*//B3LYP/6-311G* are also close to those calculated by TD-B3LYP/6-31G*//B3LYP/STO-3G. It is impractical to use such large numbers of basis functions as the former two basis sets for oligomers of larger size used; therefore, TD-B3LYP/6-31G*//B3LYP/STO-3G was employed to study the derivatives with acceptable accuracy. The excitation transition energies of the substituted PPVs by the SCLE scheme are tabulated in Table 8. The regression plots of the absorption energy of polymeric **2a**, **2b**, **3a**, and **3b** are shown in Figure 10. The excited states with the largest transition probability are also in the ^1B_u state. The absorption energy for the infinite chain of **2a**, dimethyl-substituted PPV, is 2.125 eV ($r = 0.995$) at the level of SCLE-TD-B3LYP/6-31G*//B3LYP/STO-3G. For the linear fit of the absorption energy of **2b**, dimethoxy-substituted PPV, the excited state with the largest transition probability is also ^1B_u, and thus the transition energy for the infinite chain of dimethoxy-substituted PPV is 1.647 eV ($r = 0.999$) at the same

TABLE 6: Comparison of the TD Band Gap (E_{ex}, eV) of PPV by B3LYP with Various Basis Sets[a]

scheme	polymer units (n)	TD-B3LYP/6-31G*// B3LYP/STO-3G		TD-B3LYP/6-31G*// B3LYP/6-31G*		TD-B3LYP/6-311G*// B3LYP/6-311G*	
		E_{ex}	f	E_{ex}	f	E_{ex}	f
1a	1	4.3229	0.6388	4.3485	0.6808	4.2661	0.6617
	2	3.3580	1.5068	3.3574	1.5748	3.3102	1.5547
	3	2.9180	2.2584	2.8963	2.3579	2.8609	2.3404
	4	2.6799	2.9375	2.6428	3.0689	2.6121	3.0542
	5	2.5362	3.5841	2.4875	3.7385	2.4602	3.7258
	6	2.4431	4.2206	2.3888	4.3933	2.3621	4.3827
	7	2.3836	4.8616	2.3212	5.0484	2.2960	5.0377
	∞	2.107	(0.996)	2.041	(0.995)	2.027	(0.994)

[a] The geometries are optimized at corresponding level of theory followed by the TD calculations up to the first five singlet and five triplet states. The $^1B_u \leftarrow {}^1A_g$ transitions with the largest nonzero oscillator strengths (f) are listed. The numbers in parentheses are the correlation constants (r).

TABLE 7: Comparison of the TD Band Gap (E_{ex}, eV) of Selected PPV Derivatives by B3LYP with Various Basis Sets[a]

schemes	polymer units (n)	TD-B3LYP/6-31G*// B3LYP/STO-3G		TD-B3LYP/6-31G*// B3LYP/6-31G*		TD-B3LYP/6-311G*// B3LYP/6-311G*	
		E_{ex}	f	E_{ex}	f	E_{ex}	f
2a	1	4.1909	0.3304	4.2192	0.3749	4.1348	0.4108
	2	3.2994	1.3896	3.2910	1.4433	3.2313	1.4139
	3	2.8746	2.1253	2.8462	2.2084	2.7986	2.1789
3b	1	4.1110	0.2884	4.1479	0.3253	4.0751	0.3103
	3	2.2362	1.5907	2.1844	1.5949	2.1586	1.5854

[a] The geometries are optimized at corresponding level of theories followed by the TD calculations up to the first five singlet and five triplet states. The $^1B_u \leftarrow {}^1A_g$ transitions with the largest nonzero oscillator strengths (f) are listed.

TABLE 8: SCLE-TD Band Gap (E_{ex}, eV) of PPV Derivatives (2a, 2b, 3a, and 3b) by the Restricted B3LYP Functional with 6-31G* Basis Sets Using the Geometries Optimized at the Level of B3LYP/STO-3G[a]

polymer units (n)	SCLE-TD-B3LYP/6-31G*//B3LYP/STO-3G							
	2a		**2b**		**3a**		**3b**	
	E_{ex}	f	E_{ex}	f	E_{ex}	f	E_{ex}	f
1	4.191	0.3304	4.440	0.3623	3.992	0.3603	4.111	0.2884
2	3.299	1.3896	2.971	1.1911				
3	2.875	2.1253	2.577	1.9905	2.611	1.7973	2.236	1.5907
4	2.645	2.7969	2.351	2.6960				
5	2.509	3.4338	2.212	3.3489	2.328	2.8907	1.959	2.7198
6	2.422	4.0629	2.121	3.9814				
∞	2.125	(0.995)	1.647	(0.999)	1.915	(1.000)	1.374	(0.999)

[a] These transitions with nonzero oscillator strengths (f) are $^1B_u \leftarrow {}^1A_g$ excitations. The numbers in parentheses are the correlation constants (r).

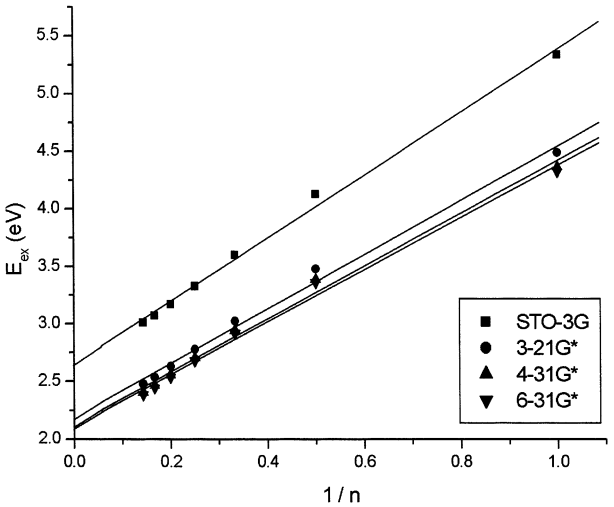

Figure 9. Excitation energy (E_{ex}, eV) of PPV (**1a**) by the SCLE-TD-B3LYP method with various basis sets. The structures are optimized at the level of B3LYP/STO-3G.

level of theory. The regression plot of the absorption spectrum of the oligomers of **3a** is the nitrile of **2a**. The most probable first excited state is also found in the ^1B_u state, and hence the transition energy for the infinite chain of this dimethyl-substituted PPV nitrile is 1.915 eV ($r = 1.000$) using the SCLE-TD-B3LYP/6-31G*//B3LYP/STO-3G theory. The least-squares fitting for the absorption energy of **3b** also gives the active excited state of the largest transition probability in the ^1B_u state. The transition energy for the polymeric chain of this dimethoxy-substituted PPV nitrile is computed to be 1.374 eV ($r = 0.999$) utilizing an identical SCLE-TD-B3LYP/6-31G*//B3LYP/STO-3G scheme. The band of nitrile **3b** lies in the near-IR region and may not be an EL polymer of industrial interest in the visible range.

Substitutions by the electron-rich functional groups are expected to generate red shifts to the observed spectra. The absorption spectra in wavelengths corresponding to PPV and the aforementioned derivatives are summarized in Table 9. The symmetric substitutions on PPV by 2n methyl groups cause an insignificant shift in the absorption spectra compared to the spectra of the original PPV (583 vs 588 nm) because of the electronically neutral property of the methyl group. Owing to the fact that the oxygen atom of the methoxy group is more electron-donating than the methyl group, the red shift caused by the methoxy group is significantly larger than the methyl group; it produces a red shift of 165 nm for the absorption. Adding more electronegative cyano groups, we find that the red shift is even larger. The nitrile of the dimethyl-substituted PPV produces a red shift of about 64 nm, whereas the corresponding nitrile of the dimethoxy-substituted PPV generages a red shift of about 150 nm. We conclude that electron-rich substitution on the PPV chain will result in a red shift of the absorption spectra—the more electron-sufficient substitution groups added, the larger the red shifts grow, possibly because of the increase in conjugated double bonds.[19]

Emission Spectra of PPV. The actual emission is estimated by analogous SCLE methodology. Density functional methods are, however, incapable of geometry optimization in designated

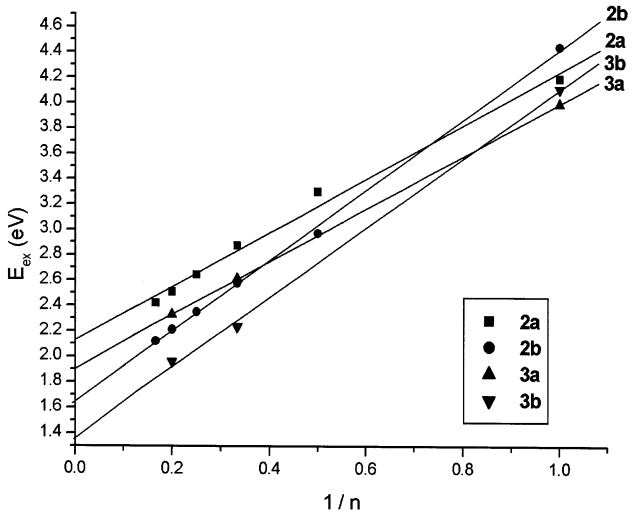

Figure 10. Excitation energy (E_{ex}, eV) of **2a**, **2b**, **3a**, and **3b** by the SCLE-TD-B3LYP method with the 6-31G* basis set. The structures are optimized at the level of B3LYP/STO-3G.

TABLE 9: Corresponding Absorption Wavelengths and Excited States of PPV and Its Derivatives by Extrapolation[a]

polymer	transition	TD excitation energy (eV)	correlation constant	corresponding wavelength (nm)
1a	$^1B_u \leftarrow {}^1A_g$	2.107	0.996	588.4
2a	$^1B_u \leftarrow {}^1A_g$	2.125	0.995	583.4
2b	$^1B_u \leftarrow {}^1A_g$	1.647	0.999	752.7
3a	$^1B_u \leftarrow {}^1A_g$	1.915	1.000	647.4
3b	$^1B_u \leftarrow {}^1A_g$	1.374	0.999	902.6

[a] The TD excitation energies are obtained at the level of SCLE-TD-B3LYP/6-31G*//B3LYP/STO-3G.

excited states because of a lack of efficient algorithms for analytical gradients. The structure in the S_1 state can be minimized by other appropriate theories such as multiconfiguration or configuration-interaction methods, and the optimal geometry is employed in the S_0 state to perform vertical TD calculations. As displayed in Figure 11, the vertical transition excited upward from the optimal geometry in the S_1 state equals the downward vertical emission ($S_0 \leftarrow S_1$). Consequently, the emission calculations are made by reoptimizations of the PPV oligomers with the CIS/6-31G* method in their first singlet excited states, followed by using the resulting geometries to perform TD calculations employing the B3LYP/6-31G* method from the singlet ground state to the first five singlet and five triplet excited states. Emission energies of PPV with nonzero oscillator strengths are found from the ^1B_u states and are listed in Table 10. These transitions corresponding to the $^1B_u \leftarrow {}^1A_g$ excitation are equivalent to the reversal emission of $^1A_g \leftarrow {}^1B_u$. The extrapolated emission energy (Figure 12) by the SCLE scheme corresponding to infinite numbers of PPV polymer is

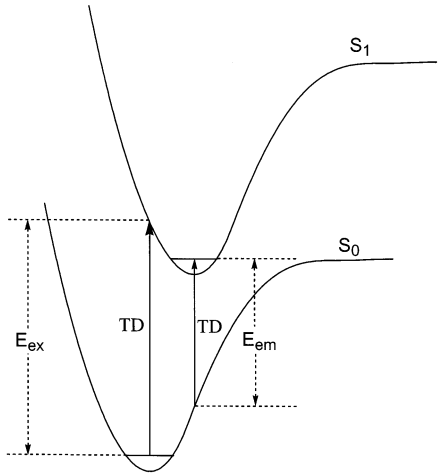

Figure 11. Using time-dependent theory for the $S_0 \leftarrow S_1$ vertical emission calculation. The optimal structure of the S_1 state is obtained with the CIS method, followed by the TD computation from the S_0 state (E_{em}).

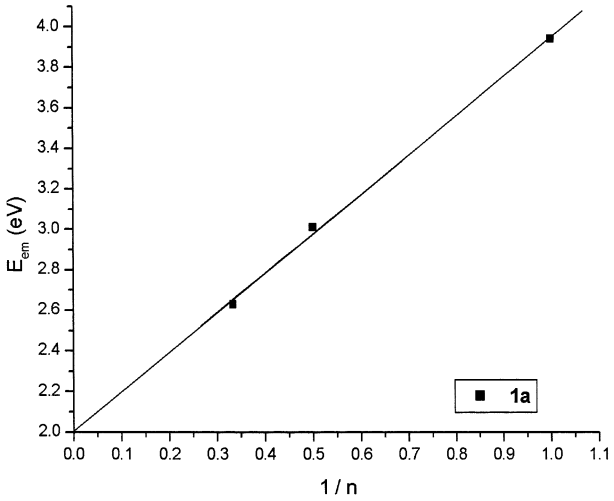

Figure 12. Emission spectrum (E_{em}, eV) of PPV (**1a**) by the SCLE-TD-B3LYP method with the 6-31G* basis set. The structures are optimized at the level of CIS/STO-3G.

2.008 eV ($r = 0.999$), converting to 618 nm, and resides on the emitting edge of the physically observed peak.[19]

By this theoretical emission, the Stokes shift of PPV is also evaluated. To conform with the available emission data in Table 10, the SCLE scheme is reperformed using solely PPV monomer through trimer and results in an excitation energy of 2.231 eV ($r = 0.997$) with the basis set of 6-31G* by B3LYP. The deviation between the excitation energy and the emission energy is 0.223 eV, which is about a 62-nm shift in the wavelength.

TABLE 10: SCLE-TD Emission Energy (E_{em}, eV) of PPV (1a) by the B3LYP Density Functional with the 6-31G* Basis Sets Using CIS Optimized Structures[a]

polymer units (n)	SCLE-TD-B3LYP/6-31G*//CIS/6-31G* emission		SCLE-TD-B3LYP/6-31G*//HF/6-31G* excitation		SCLE-TD-B3LYP/6-31G*//B3LYP/6-31G* excitation	
	E_{em}	f	E_{ex}	f	E_{ex}	f
1	3.9391	0.7129	4.4991	0.6525	4.3485	0.6808
2	3.0104	1.6533	3.5514	1.5213	3.3574	1.5748
3	2.6295	2.5146	3.1217	2.2582	2.8963	2.3579
∞	2.008	($r = 0.999$)	2.486	($r = 0.998$)	2.231	($r = 0.997$)

[a] These active transitions are $^1A_g \leftarrow {}^1B_u$ emissions with the nonzero oscillator strength (f). Similar SCLE-TD excitation energy extrapolations regarding monomer through trimer yield the theoretical Stokes shift.

Concluding Remarks

The SCLE-TD method with the hybrid B3LYP density functional is a feasible way to estimate excitation and emission transitions for infinite chains of PPV polymer as well as its derivatives by plotting corresponding excitations against the inverse of the multiple of monomeric units and extrapolating the number of units to infinity. The theoretical excitations and emissions by our modeling polymeric units are equivalent to those of the actual molecules. The conditional supplement of the terminal hydrogen atom and the $-CH=CH_2$ group is necessary to retain the molecular symmetry while utilizing the SCLE-TD scheme. Computationally, adding electron-donating substitution groups on the PPV chain generates red shifts in the spectra, which makes the prediction for theoretical color-tuning of the derivatives possible.

Acknowledgment. This work has been supported by the National Science Council of Republic of China under grants NSC 89-2113-M-007-052 and NSC 90-2113-M-007-054.

References and Notes

(1) Shirota, Y. *J. Mater. Chem.* **2000**, *10*, 1.

(2) Pope, M.; Kallmann, H. P.; Magnante, P. *J. Chem. Phys.* **1963**, *38*, 2042.

(3) Burroughes, J. H.; Bradley, D. D. C.; Brown, A. R.; Marks, R. N.; Mackay, K.; Friend, R. H.; Burn, P. L.; Holmes, A. B. *Nature* **1990**, *347*, 539.

(4) Gomes da Costa, P.; Dandrea, R. G.; Conwell, E. M. *Phys. Rev. B* **1993**, *47*, 1800.

(5) Cornil, J.; Beljonne, D.; dos Santos, D. A.; Brédas, J. L. *Synth. Met.* **1996**, *76*, 101.

(6) Dewar, M. J. S.; Zeobisch, E. G.; Healy, E. F.; Stewart, J. J. P. *J. Am. Chem. Soc.* **1985**, *107*, 3902.

(7) Pople, J. A.; Beveridge, D. L.; Dobosh, P. A. *J. Chem. Phys.* **1967**, *47*, 2026.

(8) Zerner, M. C.; Loew, G. H.; Kichner, R. F.; Mueller-Westerhoff, U. T. *J. Am. Chem. Soc.* **1980**, *102*, 589.

(9) Fröner, W.; Bogar, F.; Knab, R. *J. Mol. Struct.* **1998**, *430*, 73.

(10) Vosko, S. H.; Wilk, L.; Nusair, M. *Can. J. Phys.* **1980**, *58*, 1200.

(11) Vaschetto, M. E.; Springborg, M. *Synth. Met.* **1999**, *101*, 502.

(12) Casida, M. E.; Jamorski, C.; Casida, K. C.; Salahub, D. R. *J. Chem. Phys.* **1998**, *108*, 4439.

(13) Kwon, O.; McKee, M. L. *J. Phys. Chem. A* **2000**, *104*, 7106.

(14) Frisch, M. J.; Trucks, G. W.; Schlegel, H. B.; Scuseria, G. E.; Robb, M. A.; Cheeseman, J. R.; Zakrzewski, V. G.; Montgomery, J. A., Jr.; Stratmann, R. E.; Burant, J. C.; Dapprich, S.; Millam, J. M.; Daniels, A. D.; Kudin, K. N.; Strain, M. C.; Farkas, O.; Tomasi, J.; Barone, V.; Cossi, M.; Cammi, R.; Mennucci, B.; Pomelli, C.; Adamo, C.; Clifford, S.; Ochterski, J.; Petersson, G. A.; Ayala, P. Y.; Cui, Q.; Morokuma, K.; Malick, D. K.; Rabuck, A. D.; Raghavachari, K.; Foresman, J. B.; Cioslowski, J.; Ortiz, J. V.; Stefanov, B. B.; Liu, G.; Liashenko, A.; Piskorz, P.; Komaromi, I.; Gomperts, R.; Martin, R. L.; Fox, D. J.; Keith, T.; Al-Laham, M. A.; Peng, C. Y.; Nanayakkara, A.; Gonzalez, C.; Challacombe, M.; Gill, P. M. W.; Johnson, B. G.; Chen, W.; Wong, M. W.; Andres, J. L.; Head-Gordon, M.; Replogle, E. S.; Pople, J. A. *Gaussian 98*, revision A.11; Gaussian, Inc.: Pittsburgh, PA, 1998.

(15) Yu, J.-S. K.; Yu, C.-H. *J. Chem. Inf. Comput. Sci.* **2002**, *42*, 673.

(16) Becke, A. D. *Phys. Rev. A* **1988**, *38*, 3098. Perdew, J. P. *Phys. Rev. B* **1986**, *33*, 8822.

(17) (a) Lee, C.; Yang, W.; Parr, R. G. *Phys. Rev. B* **1988**, *37*, 785. (b) Miehlich, B.; Savin, A.; Stoll, H.; Preuss, H. *Chem. Phys. Lett.* **1989**, *157*, 200.

(18) (a) Becke, A. D. *J. Chem. Phys.* **1993**, *98*, 5648. (b) Pople, J. A.; Head-Gordon, M.; Fox, D. J.; Raghavachari, K.; Curtiss, L. A. *J. Chem. Phys.* **1989**, *90*, 5622. (c) Curtiss, L. A.; Jones, C.; Trucks, G. W.; Raghavachari, K.; Pople, J. A. *J. Chem. Phys.* **1990**, *93*, 2537.

(19) Schoo, H. F. M.; Demandt, R. J. C. E. *Philips J. Res.* **1998**, *51*, 527.